OVERVIEW OF COANDĂ JET LIFT ENHANCEMENT AND TWO-DIMENSIONAL COMPUTATIONAL STUDIES

Harijono Djojodihardjo[1] and Mohd Faisal Abdul Hamid[2]

[1]Department of Aerospace Engineering, Universiti Putra Malaysia, Selangor Darul Ehsan, Malaysia
e-mail: harijono@djojodihardjo.com

[2]Department of Aerospace Engineering, Universiti Putra Malaysia, Selangor Darul Ehsan, Malaysia

Received Date: March 12, 2012

Abstract

Motivated by attempts to enhance wind-turbine aerodynamic performance and efficiency, Coandă Jet Lift Enhancement for Circulation Control that has drawn great attention from researchers and industries is investigated numerically. Coandă Jet Circulation Control Techniques has a long history of development, although meticulous modeling and innovations for practical applications for energy conversion (such as for wind-turbine applications), aircraft wing lift enhancement and propulsion (such as for Coandă -MAV) are continually in progress. Along this line, the influence of Coandă effect for lift generation and enhancement is here investigated using two-dimensional CFD simulation. To that end, attention is focussed on Coandă jet configuration located at the trailing edge, to reveal the key elements that could exhibit the desired performance criteria for lift enhancement and drag reduction, or a combination of both. Parametric studies are carried out to obtain some optimum configuration, by varying pertinent airfoil geometrical and Coandă jet parameters. Particular attention is also given to turbulence modelling, by meticulous choice of appropriate turbulent models and scaling, commensurate with the grid generation, CFD code utilized and computational effectiveness. The present two-dimensional Coandă jet studies are carried out with wind turbine and micro-air-vehicle design in view, and discussed in the light of recent results from similar research.

Keywords: CFD, Circulation control, Coandă effect, Lift augmentation, Wind turbine

Introduction

In its simple form, Coandă Effect has been identified as the deflection of a flow near a surface following the contour of the surface, as demonstrated by Figure 1(a). Coandă effect was discovered by Henri Coandă and was patented as US Patent # 2,052,869: Device for Deflecting a Stream of Elastic Fluid Projected into an Elastic Fluid, by Henri Coandă in September 1, 1936[1]. With the progress of fluid dynamics, it has been associated with Circulation Control. Circulation control can be defined as an active flow control method for lift augmentation. Circulation control (CC) can be introduced by tangentially blowing a jet of air from a slot on the surface of a finite wing, and if introduced along the trailing edge of an airfoil or finite wing, Coandă effect may ensue which can be utilized for separation control (boundary-layer control) or super-circulation control (streamline deflection caused by jet entrainment). Circulation control is also associated with Boundary layer Control, which was defined by Gadd-El-Hak [2, 3] and others [4, 5] to include any mechanism or process through which the boundary layer of a fluid flow is caused to behave differently than it normally would were the flow developing naturally along a smooth straight surface, and belongs to flow control technology. Flow control involves

passive or active devices to effect a beneficial change in wall-bounded or free-shear flows. Whether the task is to delay/advance transition, to suppress/enhance turbulence or to prevent/provoke separation, useful end results include drag reduction, lift enhancement, mixing augmentation and flow-induced noise suppression. To enhance lift and suppress separation, various flow control techniques have been used, including rotating cylinder at leading and trailing edge [3], circulation control using tangential blowing at leading edge and trailing edge [6-7], multi-element airfoils, pulsed jet separation control, periodic excitation [8, 9], etc. The state of affairs can be summarized by Figure 1.

The progress of Computational Fluid Dynamics (CFD) has spurred renewed interest in further investigation on Coandă effect and its use to enhance lift [10- 23]. Tangential jets that take advantage of Coandă effect to closely follow the contour of the body can lead to increased circulation in the case of airfoils, or drag reduction (or drag increase if desired) in the case of bluff bodies such as an aircraft fuselage. The concept and some typical Coandă – jet applications are illustrated in Figure 2.

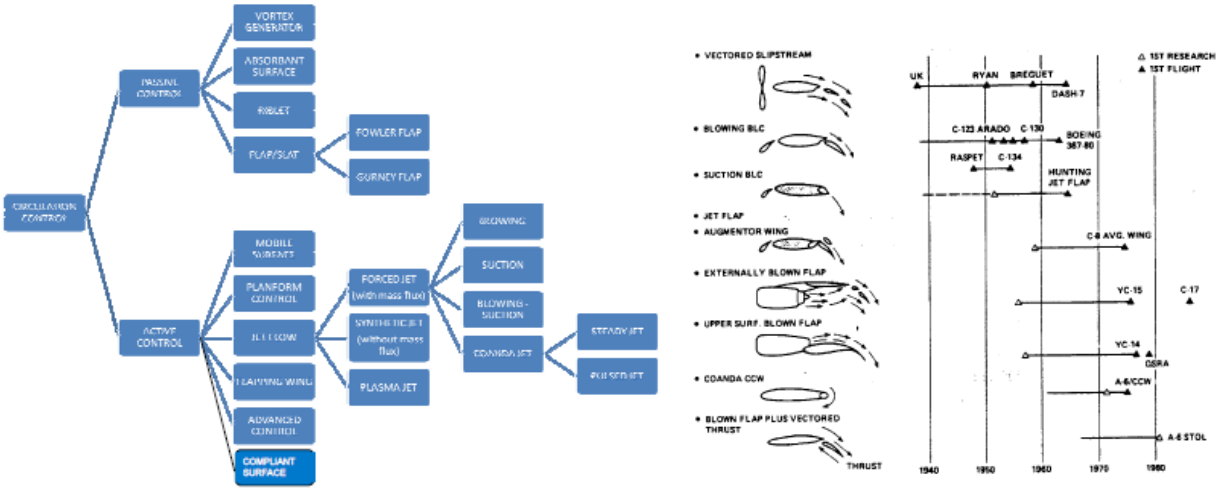

Figure 1. (a) Various methods of circulation control; **(**b**)** powered lift chronology, from synergistic airframe-propulsion interactions and integrations [11]

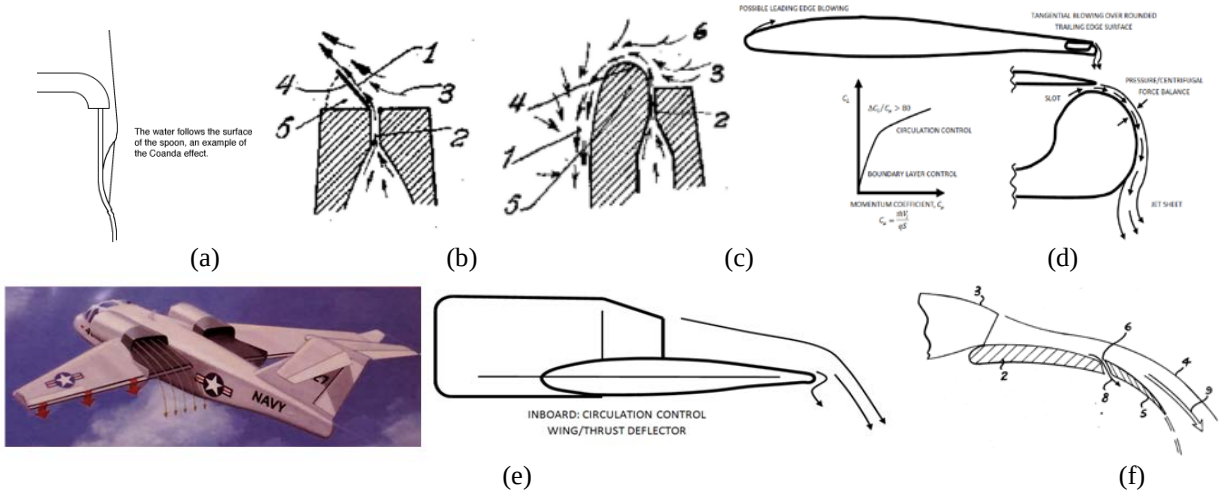

(a) (b) (c) (d)

(e) (f)

Figure 2. Coandă -effect jet concept and development: (a) simple phenomenon illustrating the Coandă principle; (b) and (c) – Coandă jet principle taken from Henri Coandă US patents 2,0052,869 [1]; (d) Coandă jet tangential blowing over trailing edge surface for lift enhancement described by Englar [10]; (e) a Navy A-6/CCW demonstrator aircraft initiated in 1968 by DTNSRDC to evaluate high lift potential [12-15], (f) One of more recent patents on Coandă Application to wings [16]

Optimizing Horizontal Axis Wind-Turbine airfoil's performance characteristics for the appropriate Reynolds number and thickness could provide additional performance enhancement in the range of 3% to 5% [24-29]. For this purpose, the concepts of circulation control through trailing edge blowing, or Coandă -jets, could be explored. Since CFD has progressed significantly and allowed numerical approaches that are based on the laws of conservation of mass, momentum, and energy in greater details, numerical simulation using CFD could be utilized to reveal and capture the physics of fluid flow behaviour near the flow boundaries, and could be useful in investigating related state of affairs of Coandă jet configured aerodynamic surfaces.

In the computational investigation of Coandă–enhanced lift for wind-turbine application, resort is made to the NREL (National Renewable Energy Laboratory) developed airfoils, To minimize the energy losses due to roughness effects and to develop special-purpose airfoils for Horizontal Axis Wind Turbine (HAWT's), the NREL (formerly the Solar Energy Research Institute -SERI), and Airfoils Inc. began a joint airfoil development effort in 1984 to produce a new series of airfoils, among others S809 airfoil [25-27], which are considered more appropriate for HAWT applications. These airfoils have been claimed to exhibit less sensitivity to roughness effects and better lift-to-drag ratios, and are recommended for retrofit blades and most new wind turbine designs [25]. In order to obtain results that can be well assessed, especially with reference to extensive research carried out as described in [19-21], S809 airfoil [24-30] is considered in the present work.

To reveal the key elements that could lead to the desired lift enhancement and drag reduction, or a combination of both., without losing generalities and furthering previous studies [31-33], the present work critically overviews Coandă jet progress and development and looks into two-dimensional to two-dimensional airfoil in subsonic flow with Coandă jet located at its trailing edge, and devotes special attention to S809 airfoil. For benchmarking, in addition to a clean S809 airfoil, the GTRI Dual Radius CCW airfoil, which has already been investigated thoroughly, is also utilized. Parametric studies are useful in obtaining general ideas on optimum configuration, and are carried out by varying pertinent airfoil geometrical and Coandă jet parameters. The numerical investigations carried out have in view applications for energy extraction system, such as wind turbine, and flight system, such as micro-air vehicles.

CFD Modeling, Grid Fineness and Turbulence Modeling

The computational studies capitalize on two-dimensional incompressible Reynolds-averaged Navier-Stokes (RANS) equation for the analysis using commercial CFD code COMSOL™ 4.2. [34]. The corresponding governing equation is given by (steady state and ignoring body forces) [35]:

$$\rho \bar{u}_j \frac{\partial \bar{u}_i}{\partial x_j} = \frac{\partial}{\partial x_j}\left[-p\delta_{ij} + \mu\left(\frac{\partial \bar{u}_i}{\partial x_j} + \frac{\partial \bar{u}_j}{\partial x_i} \right) - \rho \overline{u_i' u_j'} \right] \quad (1)$$

In order to insure good modelling of the problem and obtain plausible computational results, several key issues are critically reviewed and validated using parallel analysis based on first principles as well as using other baseline numerical computation. An analysis based on physical considerations is also carried out with reference to its application in wind-turbine blade configuration.

The choice of grid fineness in CFD turbulence modeling and obtaining the correct simulation of particular flow field is very essential. The turbulent viscosity models based on Reynolds Averaged Navier-Stokes (RANS) equations (1) are commonly employed in CFD codes due to their relative affordability [36]. An appropriate model out of a host of

available turbulence models developed to date has to be chosen. Judging from its generic clarity and user-friendliness, the $k-\varepsilon$ turbulence model is adopted, without disregarding other models that may be suitable for the purpose of the present work.

The $k-\varepsilon$ turbulence model was first proposed by Harlow and Nakayama [37, 38], in 1968, and further developed by Jones and Launder [39-42]. Continuing extensive research is carried out to understand the nature of turbulence, such as elaborated in [36-39]); various turbulence models seem to be satisfactory for only certain classes of cases. Since the choice of turbulence model and associated physical phenomena addresed are relevant in modeling and computer simulation of the flow situation near the airfoil surface, a closer look at turbulence models utilized by the CFD code chosen will be made. Although turbulence model, especially its implementation for the near-wall treatment, has been considered by some authors still to incorporate a mystery, its numerical implementation has a decisive influence on the quality of simulation results. In particular, a positivity-preserving discretization of the troublesome convective terms is an important prerequisite for the robustness of the numerical algorithm [36].

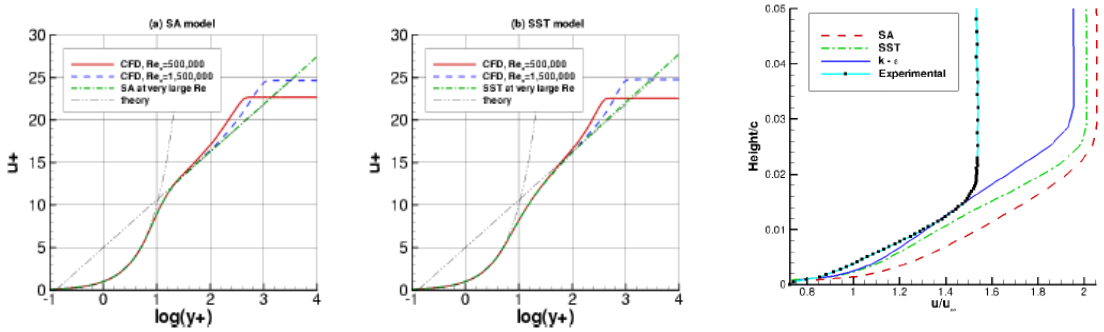

(a) *(b)*

Figure 3. (a) Typical y+ values in the turbulent boundary layer and velocity profiles in wall units for subsonic flow over flat plate, M = 0.2, Re = 1 X 106, medium grid. (Source: Menter [45]; Salim and Cheah [48]; (b) Effect of turbulence models on the upper surface, mid-chord boundary layer (M = 0.1, Re = 5.74 × 104, nozzle pressure ratio = 1.4) [49]

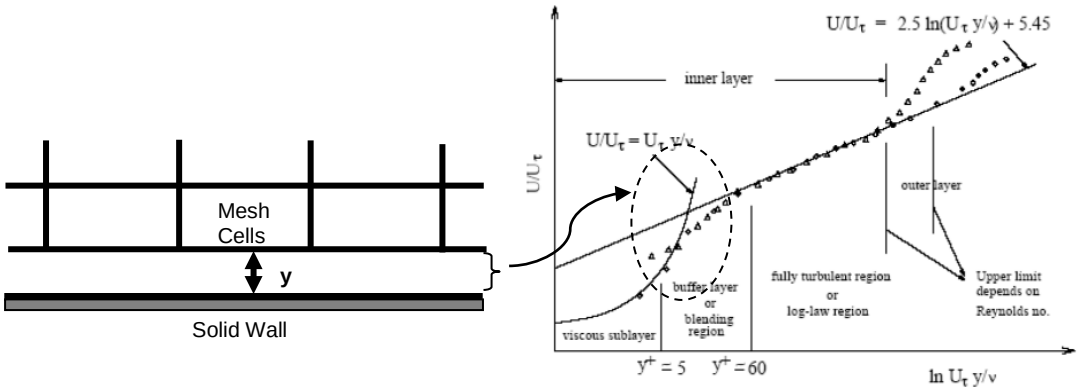

(a) (b)

Figure 4. For wall functions, the computational domain starts a distance y from the wall. (a) Depicted from COMSOL module user's guide; (b) ; (b) The structure of turbulence boundary layer, adapted from menter [45]

The $k-\varepsilon$ model introduces two additional transport equations and two dependent variables: the turbulent kinetic energy, k, and the dissipation rate of turbulence energy, ε. Turbulent viscosity is modeled by using the Komolgorov-Prandtl formula

$$\mu_\tau = \rho C_\mu \frac{k^2}{\varepsilon} \tag{2}$$

where C_μ is a model constant. The turbulent viscosity μ_τ in expression (2) was first introduced by Boussinesq [43] to draw analogy to the viscosity in laminar flow and for convenience of further analysis. The dimensionless distance in the boundary layer, sub-layer scaled, which represents the viscous sub-layer length scale, plays significant role in capturing relevant physical turbulence phenomena near the airfoil surface commensurate with the grids utilized in the numerical computation. The law of the wall can be regarded to characterize the intricate relationships between various turbulence scaling in various sublayers. The wall functions approach (wall functions were applied at the first node from the wall) uses empirical laws to model the near-wall region [36]. The law of the wall is characterized by a dimensionless distance from the wall as defined by

$$y^+ = \frac{u_\tau y}{\upsilon} \tag{3}$$

Subject to local Reynolds number considerations, the wall y+ is often used in CFD to choose the mesh fineness requirements in the numerical computation of a particular flow.

Various studies [36-46] have indicated that integration of the $k-\varepsilon$ type models through the near-wall region and application of the no-slip condition yields unsatisfactory results. Therefore, taking into account the need for effective choice of grid mesh compatible with the turbulence model adopted using the COMSOL™ 4.2. CFD code, a parametric study is carried out on two airfoils where either experimental data or computational results are available. The objective is to validate the computational procedure, turbulence model and grid size chosen and establish their plausibility for further application. The first computational nodes are placed outside the viscous sublayer. The wall functions can be used to provide near-wall boundary conditions, rather than conditions at the wall itself, for solving the momentum and turbulence transport equations without resolving the viscous sublayer and utilizing very fine mesh. The wall functions in COMSOL™ 4.2. are chosen such that the computational domain is assumed to start at a distance y from the wall, as depicted in Figures 3 and 4.

By applying the wall function at the nodes of the first computational grid meshing layer at a distance y from the wall (airfoil) surface, practically the meshing-layer of width y is removed from the computational domain, thus reducing the total number of grids involved, and hence reducing the computational time. The introduction of a wall function is intended to control the y+ value such that the y distance will not fall into the viscous sublayer. The smallest distance of y+ that can be defined, following Kuzmin [36] and Grotjans and Menter [50], corresponds to the point where the logarithmic layer meets the viscous sublayer. For this purpose, the distance y is automatically computed iteratively by solving

$y^+ = \frac{1}{k}\log y^+ + \beta = \frac{1}{0.41}\log y^+ + 5.2$, so that $y^+ = \frac{u_\tau y}{\upsilon} = \rho u_\tau \left(\frac{y}{\mu}\right)$, where $u_\tau = \rho C_\mu \frac{k^2}{\varepsilon}$ is the friction velocity, and is equal to 11.06 [36].

If the mesh is relatively coarse, y^+ can become higher than 11.06. Therefore, care is exercised in the choice of grids in the vicinity of the airfoil surface, to obtain a certain acceptable error tolerance, including those contributed by numerical error and uncertainties. The plausibility of the numerical results will be judged by comparison to other established numerical or experimental results for specific cases.

Grid Generation

Computational Grid

In the present work, the grids were constructed following free mesh parameter grid generation using an algebraic grid generator and varied from extremely coarse up to extremely fine grids in a structured fashion. Near the surface of the airfoil, boundary-layer based meshing is carried out throughout following Table 1.

Table 1. Computational Grid Meshing-layer Properties

Parameter	Range
Number of mesh layers in the boundary layers	8
Boundary layer mesh stretching factor	1.2
Thickness of first mesh layer	0.00005 – 0.0002
Thickness adjustment factor	1

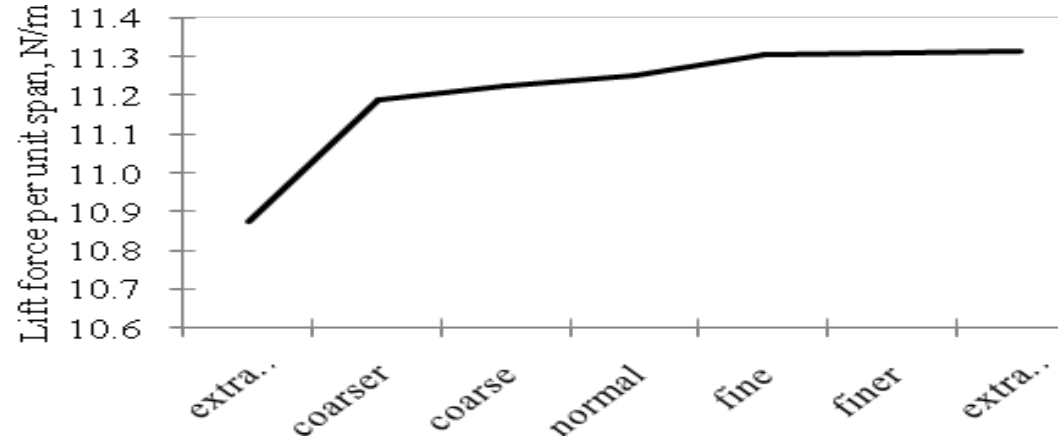

(a)

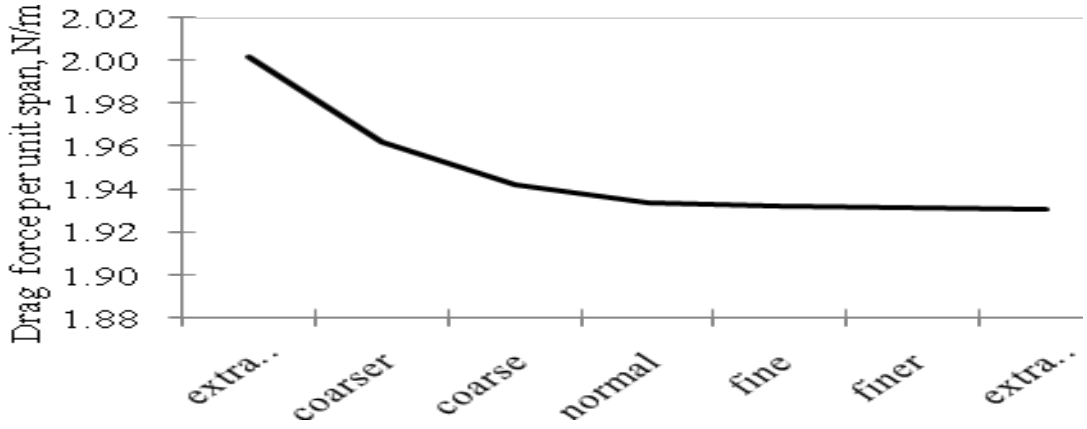

(b)

Figure 5. Grid sensitivity study for clean S809 airfoil at zero degree angle of attack (a) Lift force per unit span (b) Drag force per unit span

Having chosen the thickness of the elements of the first meshing layer adjacent to the airfoil surface, the following consecutive layers were stretched with a stretching factor of 1.2, for eight consecutive layers. The thickness adjustment factor in the computation using COMSOL™ 4.2. was chosen to be one, as shown in Table 1. Grid sensitivity study on the lift and drag forces per unit span for clean airfoil at zero angle of attack [34], as illustrated in Figure 5, indicates that the choice of grid size in the range of *fine* up to *extra fine* grid size are acceptable, since within this range the lift as well as the drag forces does not change appreciably.

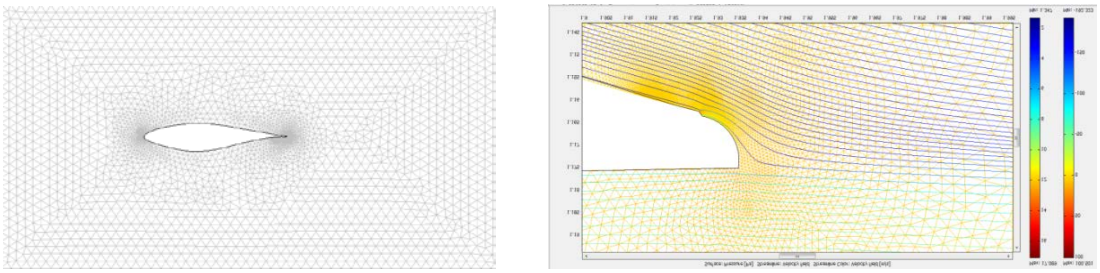

(a) (b)

Figure 6. (a) Computational Grid around a Typical Airfoil, here shown for S809 Airfoil (b) Detail of a typical flow field in the vicinity of the Coandă jet near the trailing edge

In order to control the grid size not to be excessive, in the present example the first meshing layer outside the viscous sublayer in the boundary layer was set to be in the order of 0.005 m, while at the TE rounding-off surface the maximum element size was set at 0.001 m.

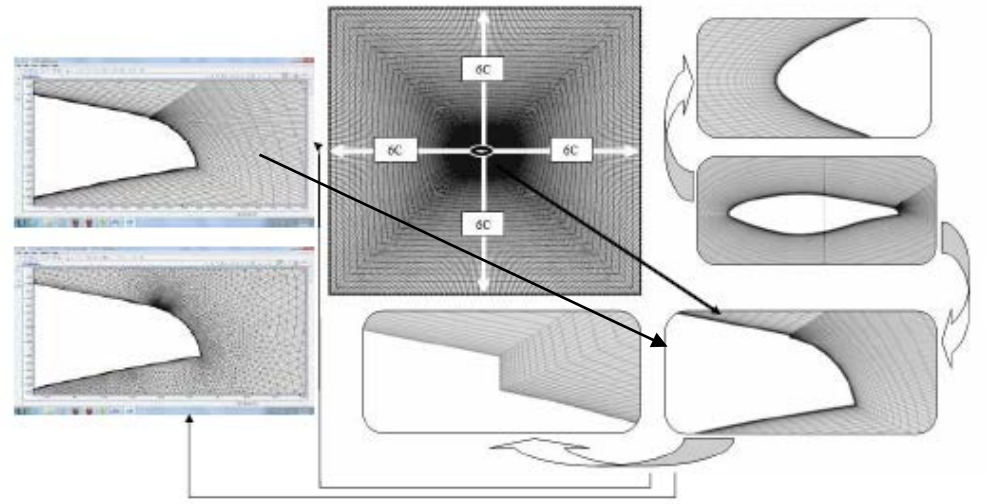

Figure 7. Computational grid around a typical airfoil, shown here for S809 airfoil, indicating careful choice of grid generation in the vicinity of Coandă jet near the trailing edge

At the Coandă jet outlet, the surface is divided into a minimum of 10 grid meshes. Along with the requirement of the y+ value to capture the salient turbulent flow field sublayers, a range of values of the grid dimension could be chosen to represent the thickness of the first meshing sublayers. In the presentexample the grid dimension waschosen to be between

0.00005 m – 0.0002 m, commensurate with the curvature on the airfoil surface. The grid generator is sufficiently general so that one can easily vary the jet slot location and size.

Grid spacing and clustering can have significant effects on wind turbine load and performance predictions [29, 47]. The outer boundary is placed far away from the blade surface, at least at six chord lengths (6C) from the airfoil surface, to avoid significant influence from outer boundary into the interior domain. The computational domain and the grid in the vicinity of the airfoil surface and Coandă jet are exhibited in Figures 6 and 7.

Computational Domain

In carrying out the computation using CFD Code COMSOL™ 4.2., the initial conditions are set to be equal to the properties of the free-stream flow condition. The flow properties everywhere inside the flow field are assumed to be uniform and set to the free-stream values. The following initial values are used:

$$u = u_\infty, \qquad v = v_\infty \qquad \rho = \rho_\infty$$
$$p = p_\infty \qquad T = T_\infty \tag{4}$$

The outer boundary is placed far away from the airfoil surface, at a minimum distance of 6 chord lengths (6C). Free-stream boundary conditions are applied at the outer boundaries of the computational domain. The jet is set to be tangential to the blade surface at the Coandă jet nozzle location. The jet velocity profile is specified to be uniform at the jet exit. On the airfoil surface, except at the jet exit, no-slip boundary conditions are applied. To gain the benefits of the Coandă - jet, the jet velocity should be designed to be larger than the potential flow velocity at the vicinity of the outer edge of the boundary layer. In addition, the thickness of the Coandă jet should be designed to be less than the local boundary layer thickness.

Validation

Various baseline cases have been investigated using similar computational procedure, prior to its utilization for parametric study, with favorable results. For benchmarking purposes the code has been applied to calculate the lift-slope characteristics of S809 airfoil (clean configuration, without Coandă) and GTRI CCW Dual Radius airfoil (with Coandă), and compared to the results obtained by Somers [43] and Englar et al [3] respectively. The results as shown in Figures 8 and 9 demonstrated its plausibility for the present investigation.

Computational results exhibited in Figure 4 served to validate the computational procedure associated with the use of COMSOL™ 4.2. code in the numerical simulation and as a baseline in furthering the computational study of Coandă jet in the present study. Figure 8 compares the present computational simulation using $k-\varepsilon$ turbulence model and Kuzmin's [29] wall function with the experimental data of Somers [51]. The numerical computation simulates similar experimental conditions of Somers for clean S809 airfoil (with wall boundary conditions and without Coandă jet). It also shows that the lift and drag coefficient at zero angle of attack are in close agreement with the experimental data. Similar numerical simulation was carried out for GTRI Dual Radius CCW airfoil with leading edge blowing. Figure 9 compares the results to the experimental data of Jones and Englar [13] with the same boundary conditions and jet configuration using $k-\varepsilon$ turbulence model and Kuzmin's wall function. Of significant interests are the grid size, the wall function and y+ value utilized for numerical simulation. The associated y value for the cells adjacent to the airfoil surface was designed to be no more than 0.0002m in order to satisfy the y+ value requirements, which were chosen to be 11.06. The results exhibited in Figure 8 for this case is also encouraging due to the close agreement between the present computation and the experimental data.

The results exhibited in both examples above serve to indicate, that the computational procedure and choice of turbulence model seem to be satisfactory, and could lend support to further use of the approach in the numerical parametric study.

All computations in the present study were performed on a laptop computer with a 2.10 GHz Intel Core Duo processor, 4 GB of RAM, and 32-bit Operating System. Typical computation time for the computation of the flow characteristics around a two dimensional airfoil is in the order of 4 hours with around 300,000 degrees of freedom by using stationary segregated solver in $k-\varepsilon$ turbulent model analysis.

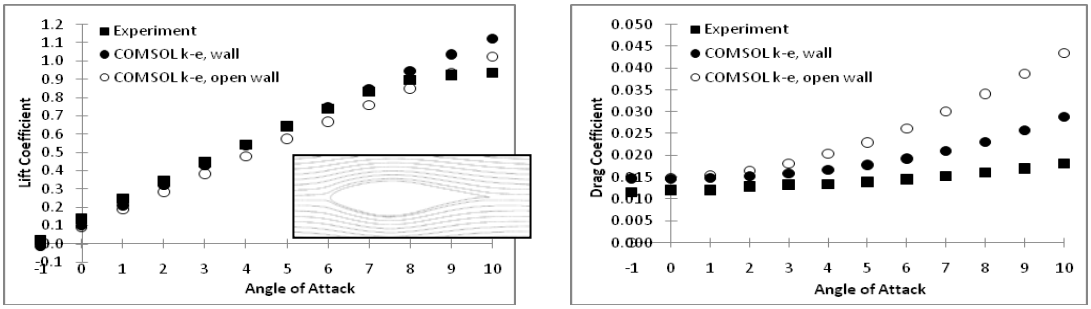

(a) *(b)*

Figure 8. Comparison for validation of S809 airfoil of CFD computational results using COMSOL™ 4.2. k-e turbulence model and experimental values from Somers (NREL [51]) at Re = 1E6 (a) Lift coefficient (b) Drag coefficient

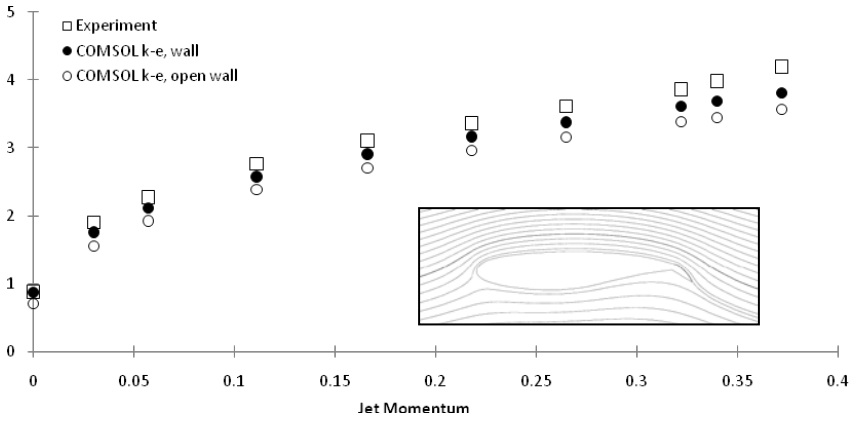

Figure 9. Comparison of lift-curve slope for GTRI Dual Radius CCW airfoil with LE blowing on CFD computation using COMSOL™ 4.2. k-e turbulence model and experimental values from Englar et al [13] at Re = 395,000

Results and Discussions

Coandă Jet Design Configuration

For the purpose of assessing the influence and the effectiveness of the Coandă enhanced lift on wind-turbine blade, a generic two-dimensional study is carried out. The problem at issue is how the Coandă jet can be introduced at the trailing edge of the airfoil, bearing in mind that such design may recover any losses due to the possible inception of flow separation there. In addition, for effective Coandă jet performance, a curvature should be introduced.

Furthermore, the thickness of the Coandă jet as introduced on the airfoil surface could have a very critical effect on the intended lift enhancement function. For best effect, the lower surface near the trailing edge should be flat, as suggested by Tongchitpakdee [18-19]. The design of the Coandă-configured trailing edge should also consider the off-design conditions. With all these considerations, a configuration suggested is exhibited in Figure 10. This figure illustrates the initial airfoil shape in the vicinity of the trailing edge, and the final airfoil shape there. With the pressure distributions for all cases obtained by running COMSOLE ® CFD code. The iteration process required the geometry to be remeshed and a new CFD solution to be obtained.

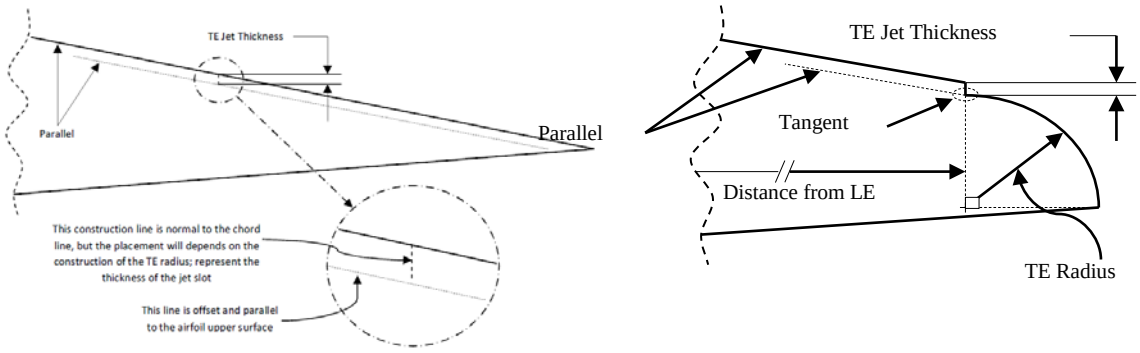

(a) (b)

Figure 10. Trailing edge construction of the Coandă configured airfoil (the jet flow is tangential to the rounded circular sector) (a) initial configuration (b) final configuration

S809 Airfoil Computational Results

Next, we would like to investigate the influence of specifically designed airfoil geometry for wind turbine application, and for this purpose a typical S809, in clean and Coandă jet equipped configurations. S809 airfoil represents one of a new series of airfoils which are specifically designed for HAWT applications [25-27]. For the present study, the numerical simulation was carried out at two free-stream velocities. These are 5.77m/s (corresponding to Re = 3.95 x 10^5) and 14.6 m/sec (corresponding to Re = 1 x 10^6), which represent low and high free-stream cases, respectively, while the chord-length is maintained at c = 1m, and density at ρ = 1.225 kg/m^3. The baseline for assessing the advantages of Coandă jet from parametric study on S809 airfoil is the computational result for the clean airfoil. The computational result for this baseline case has been validated by comparison of the computational value for the same S809 airfoil to the experimental results based on wind-tunnel test.

The two-dimensional numerical simulation study for the S809 airfoil is carried out in logical and progressive steps. First, the numerical computation is performed on the clean S809 airfoil, then on the Coandă jet configured S809 airfoil without the jet (i.e. after appropriate modification due to TE rounding-off and back-step geometry), and then finally on Coandă jet configured S809 airfoil in its operational configuration.

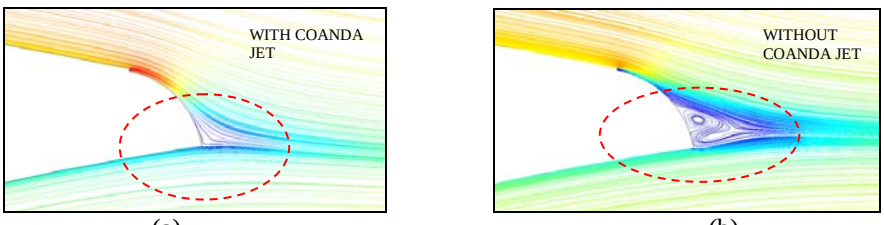

(a) (b)

Figure 11. Flow Fields of S809 airfoil (a) with, and (b) without - Coandă -jet

To address three dimensional wind-turbine configurations, particularly for the optimum design of a Horizontal Axis Wind-Turbine (HAWT), logical and physical adaptation should be made, taking into account the fact that different airfoil profiles may be employed at various radial sections. Certain assumptions have to be made in order to project the two-dimensional simulation results to the three-dimensional case, which may be necessary to evaluate the equivalent Betz limit.

The flow fields in the vicinity of the trailing edge for both configurations are shown in Figures 11a and 11b. Careful inspection of these figures may lead to the identification of the geometry of the flow that could contribute to increased lift, in similar fashion as that contributed by flap, jet-flap or Gurney flap. Figure 11b typifies the flow field around Coandă configured S809 airfoil without Coandă jet (only with its back-step configuration), for further reference.

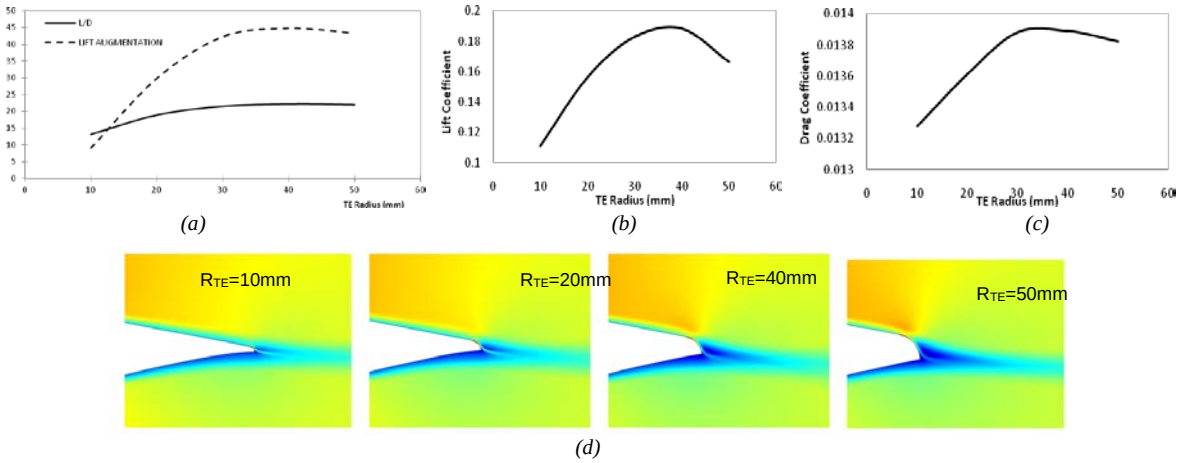

Figure 12. (a) The effect of TE radius on L/D with Coandă-jet (b) Lift coefficient (c) Drag coefficient; (Re =1 x10^6) (d) Velocity flow field for different TE radius; $C_\mu = 0.005$, t_{jet} = 1 mm)

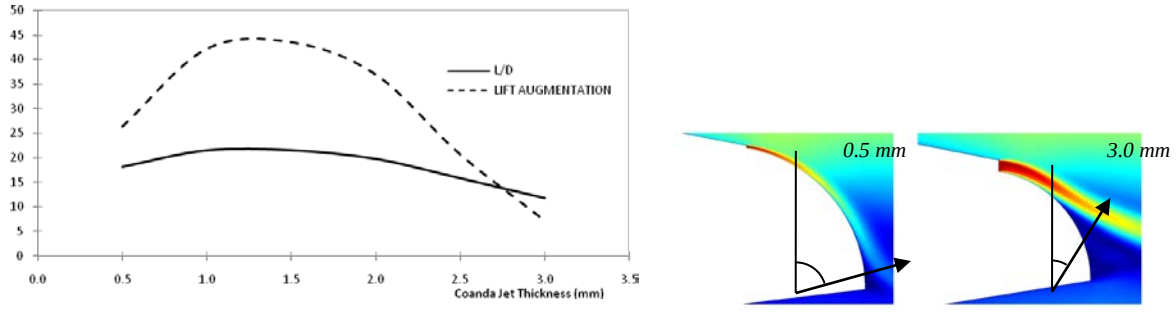

Figure 13. (a) The effect of jet thickness on the L/D and lift augmentation (b) Flow separation with different Coandă jet thickness (Re = 1 x 10^6, R = 10 mm $C_\mu = 0.005$,)

The trailing edge radius plays an important role in the Coandă configured design airfoil, since it may positively or negatively influence the downstream flow behavior. Thongcitpakdee [28-29] had claimed that the lower surface at the TE of the applied Coandă jet should be flat in order to minimize the drag when the jet is turned off.

Also, as reported earlier by Abramson and Rogers [52-53] in the late 1980's, in spite of ability to generate more lift, the technique has not in general been applied to production aircrafts. Many of the roadblocks have been associated with the engine bleed requirements and cruise penalties associated with blown blunt trailing edges. In addition, there is a tradeoff between the use of a larger radius Coandă -configured airfoil for maximum lift and a smaller radius one for minimum cruise drag.

In contrast to the needs of trailing edge rounding-off radius, performance degradation associated with it always stands as an issue due to the drag penalty when the jet is in the off mode. To overcome such draw-back, the TE radius should be specificallly and carefully designed. For that purpose, simulations at several TE radius (from 10mm to 50mm) have been performed, at a fixed Coandă jet momentum coefficient C_μ ($C_\mu = 0.003$, considered just enough to fit with the wind turbine application), and at a constant free-stream velocity of $V_\infty = 14.6 \ m/sec$ (Re= 1 x 10^6), to investigate the effect of TE radius on the aerodynamic characteristics of Coandă configured airfoils.

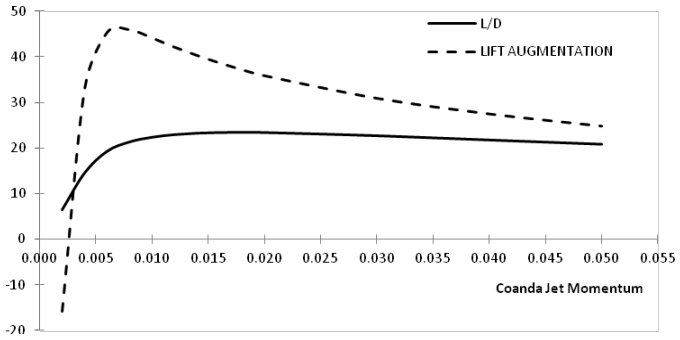

Figure 14. The effect of jet momentum on the L/D and lift augmentation (Re = 3.95 x 10^5, R_{TE} = 50 mm, t_{jet} = 1 mm)

Results exhibited in Figure 12 show that a higher L/D can be achieved with a smaller TE radius (30 mm), and that the L/D is decreasing as the TE radius is increased from 30 mm to 50 mm. The effect of TE radius on the lift augmention does not seem to be significant, as exhibited by the dashed line in Figure 8a. However, when the TE radius is increased beyond certain value (in Figure 8, >> 35 mm), the TE rounding-off seems to be ineffective, even detrimental.

Variation of the Coandă jet thickness from 0.5 mm to 3.0 mm at a fixed C_μ ($C_\mu = 0.005$), and at a constant free-stream velocity of $V_\infty = 14.6 \ m/sec$ (Re= 1 x 10^6) is performed to investigate the effect of Coandă jet thickness (also called jet-slot-thickness) on the aerodynamic characteristics of Coandă configured airfoils. From Figure 13, it is found that a higher L/D can be achieved with a smaller Coandă jet thickness (1.0-1.5 mm), and that the L/D is decreased rapidly as the Coandă jet thickness is increased from 1.0 mm to 3.0 mm. A similar behavior is observed for the lift augmention as exhibited by the dashed line in Figure 13. However, generating a smaller jet requires higher pressure than a larger one at the same momentum coefficient. Since higher lift with as low mass flow rate as possible is preferred, a thin jet is more beneficial than a thick jet. From aerodynamic design perspective, within the range of agreeable power to generate Coandă -jet, a smaller Coandă jet thickness is preferred, although further careful trade-off study should be made. The

performance of Coandă configured airfoils is dependent on the jet momentum conditions, which are important driving parameters. Figures 14 shows numerical simulation for a free-stream velocity of 5.77 m/sec.

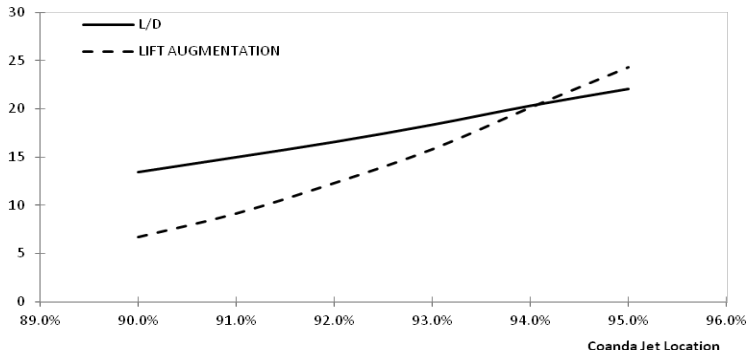

(a)

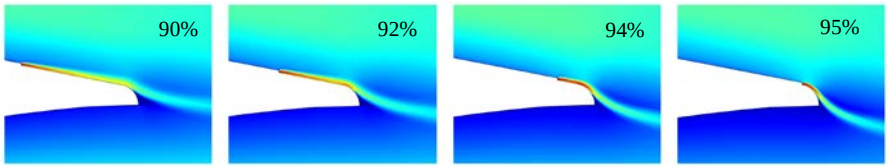

(b)

Figure 15. (a) The effect of Coandă jet location on the L/D and lift augmentation (b) Velocity flow field for different Coandă jet location (Re = 1 x10^6, R_{TE} = 10 mm, t_{jet} = 1 mm, $C_\mu = 0.010$)

At very low jet momentum coefficient $C_\mu << 0.005$, the jet velocity is too low to generate a sufficiently strong Coandă effects that eliminates separation and vortex shedding. The lift to drag ratio L/D increases significantly with the increase of the jet momentum coefficient (C_μ) until the jet momentum coefficient reaches $C_\mu > 0.01$. After this value, the effect is otherwise. Under fixed free-stream velocity and fixed Coandă jet thickness, the total mass flow rate increases linearly with the increase of the jet momentum. Also the jet velocity ($V_{Coandă\ jet}$) has to be increased with the mass flow rate to keep a constant C_μ. The dotted line shown in Figure 14 shows that the maximum lift augmention is slightly above 60.

Contribution of Coandă Jet Momentum to Wind-Turbine Power

It should be noted that for the purposes of the present work, a uniform jet velocity profile has been adopted; this could be readily modified for more realistic modeling or design requirements. Numerical results indicate that there exists an optimum Coandă jet configuration, which has been the subject of parametric study as exhibited in Figures 8 – 11 for S809 airfoil. A significant design parameter for boundary condition, which has been utilized to characterize Coandă jet application by many investigators [10-15, 18-20], is specified by the momentum coefficient of the jet, C_μ.

For two-dimensional modeling, an equivalent jet momentum coefficient C_μ^* can be defined as:

$$C_\mu^* \equiv \frac{\dot{m}_{Coandajet} V_{Coandajet}}{\frac{1}{2}\rho V_\infty^2 A_{refairfoil}} \equiv \frac{\rho_{Coandajet} V_{Coandajet}^2 t_{Coandajet}}{\frac{1}{2}\rho_\infty V_\infty^2 c} \quad (5)$$

This expression shows that for a given constant C_μ, changing the thickness of the Coandă jet will affect C_μ favorably.

To justify the results of the present study, and to give us a physical explanation of the effect of Coandă -jet, one may attempt to carry out simple calculation using first principle and Kutta-Joukowski law for potential flow, and compare the Lift of the Coandă jet configured airfoil with the clean one obtained using COMSOL™ 4.2. CFD code.

$$L_{CoandajetAirfoil} = L_{cleanAirfoil} + \rho_\infty \left(V_{Coandajet} - V_\infty \right) h_{Coandajet} \quad (7)$$

where $h_{Coandajet}$ is the moment arm of the Coandă jet with respect to the airfoil aerodynamic center. One then may arrive at a very good conclusion on the contribution of the Coandă jet to the lift (surprisingly, using COMSOL™ 4.2. CFD results for the lift ($L_{CoandajetAirfoil}$) values, the accuracy obtained by using equation (3) was in the order of 1.39%). However, care should be exercised to insure valid modeling for comparison.

For the three-dimensional configuration, there is a physical relationship between the Wind-Turbine shaft torque (which is a direct measure of the shaft power extracted) with C_μ, and in the actual three-dimensional case, the wind-turbine rotor yaw angle [28-29]. From the numerical results gained thus far, it can be surmised that circulation control, which in this particular case obtained by utilizing Trailing-edge Coandă -jet, can considerably increases the torque generated through the L/D increase gained.

The maximum theoretical power that can be extracted from the free stream (ambient air) is given by the Betz limit:

$$P_{Betz} = \frac{8}{27} \rho A_{Wind-turbine\ rotor} V_\infty^{\ 2} \quad (6)$$

(where V_∞ is the free-stream wind speed). With the use of Coandă -jet, assuming the jet energy can be drawn from the inner part of the free-stream in the vicinity of the wind-turbine rotor hub, the Coandă jet additional power output corresponding to the jet momentum coefficient should contribute to the increase of shaft power output given by the theoretical Betz limit. Tongchitpakdee studies [28] also indicated such results. It should be noted that the ambient air free-stream wind speed V_∞ for the Wind-Turbine is different from the V_∞ implied in the present two-dimensional parametric study, which is the resultant of the ambient-air wind speed and the rotational speed of the particular section of the rotor blade.

Conclusions

CFD numerical experiments have been carried out to elaborate work reported earlier [25-27], with the objective to verify the favorable effects of Coandă -configured airfoil for enhanced aerodynamic performance and obtain some guidelines for the critical features of Coandă jet configured airfoil. Care has been exercised in the choice of turbulence model and other relevant parameters commensurate with the grid fineness desired, in particular since the number of grid utilized is relatively small in view of the desk-top computer utilized capabilities. Comparison of the numerical computation results for some baseline cases with experimental data under similar conditions lends support to the present computational parametric study.

The results show that the introduction of Coandă jet on S809 Coandă configured airfoil carried out in the present work confirms its effectiveness in enhancing L/D, which depends on the jet velocity. Rounding-off of the TE along with the introduction of the

Coandă jet seems to be effective in increasing L/D in airfoil specifically designed for Wind-Turbine, here exemplified by S809. Within the limits of local boundary layer thickness, there is a certain range of effective and optimum Coandă jet thickness commensurate with the airfoil dimension. With specific design specifications related to the Coandă jet thickness and TE rounding-off size, the Coandă jet momentum needed to improve the performance (lift augmentation due to jet) should not be excessive but sufficient to delay separation until the tip of the TE (where the upper surface meets the lower one). In addition, the Coandă jet should be placed sufficiently close to the TE to avoid premature separation.

Numerical results presented have been confined to zero angle-of-attack case, which has been considered to be very strategic in exhibiting the merit of Coandă jet as lift enhancer. The numerical studies could be extended to increasing angle of attack to obtain more comprehensive information, for which the choice of turbulence model will be more crucial.

Acknowledgements

The authors would like to thank Universiti Putra Malaysia (UPM) for granting Research University Grant Scheme (RUGS) No. 05-02-10-0928RU, CC-91933, under which the research is initiated and Ministry of Higher Education for granting Exploratory Research Grant Scheme Project Code: ERGS 5527088, under which the research is carried out. The corresponding author would also like to thank Universitas Al-Azhar Indonesia for the opportunity to carry out the present research at Universiti Putra Malaysia.

Nomenclature

CFD	Computational Fluid Dynamic
CCW	Circulation Control Wing
R	Trailing edge radius (mm)
C	Airfoil chord length (m)
L	Lift force (N)
D	Drag force (N)
H	Coandă jet thickness (mm)
L/D	Lift over drag ratio
R/C	Trailing edge radius over airfoil chord length ratio
H/C	Coandă jet thickness over airfoil chord length ratio
TE	Trailing Edge
STOL	Short Takeoff Landing
y^+	Dimensionless wall distance for a wall-bounded flow
u_τ	Friction velocity
y	Distance to the nearest wall
ν	Kinematic viscosity
τ_w	Wall shear stress
ρ	Density
μ_τ	Turbulent Viscosity, as defined by Equation (2)
HAWT	Horizontal Axis Wind Turbine
M	Mach number
C_μ	Turbulent Model Constant, as defined by Equation (2)

C_μ	Momentum coefficient
$\frac{\Delta C_L}{C_L}$	Lift augmentation
MW	Megawatt
MWh	Megawatt hour

References

[1] H. Coandă, *Coandă Effect,* US Patents 2,052,869, 1936, [Online]. Available: http:// www.rexresearch. com/Coandă /1Coandă.htm

[2] M. Gad-el-Hak, "Modern developments in flow control," In: *Applied Mechanics Reviews*, Vol. 49, pp. 365–379, 1996.

[3] M. Gad-el Hak, *Flow Control: Passive, Active, and Reactive Flow Management*, Cambridge University Press, 2000.

[4] M.H. Shojaefard, A.R. Noorpoor, A. Avanesians, M. Ghaffarpour, "Numerical Investigation of Flow Control by Suction and Injection on a Subsonic Airfoil," *American Journal of Applied Sciences 2*, Vol. 10, pp. 1474-1480, 2005.

[5] L.D. Kral, "Active Flow Control Technology," *ASME Fluids Engineering Technical Brief*, 2000.

[6] G.-C. Zha, W. Gao, and C.D. Paxton, "Jet effects on co-flow jet airfoil performance," *AIAA Journal*, Vol. 45, No. 6, June 2007.

[7] G.-C. Zha, B.F. Carroll, C.D. Paxton, C.A. Conley, and A. Wells, "High performance airfoil using co-flow jet flow control," *AIAA Journal*, Vol 45, No. 8, pp. 2087-2090, 2007

[8] G.S. Jones, R.J. Englar, "Advances in pneumatic-controlled high-lift systems through pulsed blowing," *AIAA 2003-3411*, 21st AIAA Applied Aerodynamics Conference, Orlando, Florida, 23-26 June 2003.

[9] K. Taira, and C.W. Rowley, "Lift enhancement for low-aspect-ratio wings with periodic excitation," *AIAA Journal*, Vol. 48, No. 8, August 2010.

[10] R.J. Englar, *Advanced Aerodynamic Devices to Improve the Performance, Economics, Handling and Safety of Heavy Vehicles*, SAE Technical Paper Series 2001-01-2072, 2001.

[11] S.E. Yaros, M.G. Sexstone, L.D. Huebner, J.E. Lamar, R.E. McKinley, Jr., A.O. Torres, C.L. Burley, R.C. Scott, and W.J. Small, *Synergistic Airframe-Propulsion Interactions and Integrations: A White Paper Prepared by the 1996-1997 Langley Aeronautics Technical Committee*, NASA/TM-1998-207644, 1998.

[12] M.J. Harris, *Investigation of the Circulation Control Wing/Upper Surface Blowing High-Lift System on a Low Aspect Ratio Semispan Model*, Report DTNSRDC/ ASED-81/10, David Taylor Naval Ship R&D Center, Aviation and Surface Effects Department, Bethesda, Maryland 20084, 1981.

[13] R.J. Englar, *Low-Speed Aerodynamic Characteristics of a Small, Fixed- Trailing-Edge Circulation Control Wing Configuration Fitted to a Supercritical Airfoil*, DTNS RDC/ASE D-81/08, David Taylor Naval Ship R&D Center, Aviation and Surface Effects Department, Bethesda, Maryland 20084, 1981.

[14] R.J. Englar, M.J. Smith, S.M. Kelley, and R.C. Rover, "Application of circulation control to advanced subsonic transport aircraft, Part I: Airfoil development," *Journal of Aircraft*, Vol. 31, No. 5, pp. 1160-1168, 1994.

[15] R.J. Englar, M. J. Smith, S.M. Kelley, and R.C. Rover, "Application of circulation control to advanced subsonic transport aircraft, Part II: Transport application," *Journal of Aircraft*, Vol. 31, No. 5, pp. 1169-1177, 1994.

[16] C. Grotz, *Boundary layer scoop for the enhancement ofCoandă Effect flow deflection over a wing/flap surface*, US Patent US4146197, 27 March 1979.
[17] Y.G. Zhulev, and S.I. Inshakov, "On the possibility of enhancing the efficiency of tangential blowing of a slit jet from an airfoil surface," *Fluid Dynamics*, Vol. 31, No. 4, pp. 631-634, 1996 (Translated from Izvestiya Rossiiskoi Akademii Nauk, Mekhanika Zhidkosti i Gaza, no. 4, pp. 182-186, July-August, 1996).
[18] R. Radespiel, K.C. Pfingsten, C. Jensch, "Flow analysis of augmented high–lift systems," In: *Hermann Schlichting – 100 Years: Scientific Colloquium Celebrating the Anniversary of His Birthday, Braunschweig, Germany 2007*, R. Radespiel, C-C Rossow, and B.W. Brinkmann, eds.: Springer–Verlag Berlin Heidelberg, pp. 168 – 189, 2009.
[19] Y. Liu, L.N. Sankar, R.J. Englar, and K. Ahuja, *Numerical Simulations of the Steady and Unsteady Aerodynamic Characteristics of a Circulation Control Wing*, AIAA 2001-0704, the 39th AIAA Aerospace Sciences Meeting, Reno, NV, 2001.
[20] Y. Liu, *Numerical Simulations of the Aerodynamic Characteristics of Circulation Control Wing Sections*, Thesis (PhD), Georgia Institute of Technology, May 2003.
[21] J. Wu, L.N. Sankar, S. Kondor, "Numerical modelling of Coandă jet controlled Nacelle configuration," Paper AIAA-2004-0228, In: *42nd AIAA Aerospace Science Meeting and Exhibit*, Reno, Nevada, 5-8 January 2004.
[22] M. Mamou, and M. Khalid, "Steady and unsteady flow simulation of a combined jet flap and Coandă jet effects on a 2D airfoil aerodynamic performance," In: *Revue des Energies Renouvelables CER'07 Oujda*, pp. 55-60, 2007.
[23] T. Nishino, S. Hahn, and K. Shariff, "Large-eddy simulations of a turbulent Coandă jet on a circulation control airfoil," *Physics of Fluids*, Vol. 22 No. 12, 2010.
[24] G. Xu, *Computational Studies of Horizontal Axis Wind Turbines*, Thesis(PhD), School of Aerospace Engineering, Georgia Institute of Technology, Atlanta, Georgia, 2001.
[25] J.L. Tangler, B. Smith, and D. Jager, *SERI Advanced Wind Turbine Blades*, NREL/TP 257-4492, UC Category: 261, DE92001216, National Renewable Energy Laboratory, Colorado, 1992.
[26] J.L. Tangler, and D.M. Somers, *NREL Airfoil Families for HAWTs*, American Wind Energy Association, NREL/TP-442-7109, UC Category: 1211, DE95000267, 1995.
[27] E.P.N. Duque, W. Johnson, C.P. van Dam, R. Cortes, and K. Yee, *Numerical Predictions of Wind Turbine Power and Aerodynamic Loads for the NREL Phase II Combined Experiment Rotor*, AIAA-2000-0038, the 38th AIAA Aerospace Sciences Meeting, Reno, Nevada, 2000.
[28] C. Tongchitpakdee, *Computational Studies of the Effects of Active and Passive Circulation Enhancement Concepts on Wind Turbine Performance*, Thesis(PhD), Georgia Institute of Technology, August 2007.
[29] C. Tongchitpakdee, S. Benjanirat, and L.N. Sankar, "Numerical studies of the effects of active and passive circulation enhancement concepts on wind turbine performance," *Journal of Solar Energy Engineering, Transactions of the ASME*, Vol. 128, pp. 444, 2006.
[30] G. Xu, and L.N. Sankar, "Computational study of horizontal axis wind turbines," *UASME Journal of Solar Energy Engineering*, Vol. 122, No. 1, pp. 35-39, 2000.
[31] M.F. Abdul-Hamid, H. Djojodihardjo, S. Suzuki, and F. Mustapha,"Numerical assessment of Coandă effect as airfoil lift enhancer in wind-turbine configuration," In: *Proceedings of Regional Conference on Mechanical and Aerospace Technology*, Bali, February 9-10, 2010.

[32] H. Djojodihardjo, and M.F. Abdul Hamid, "Review and numerical a nalysis of Coandă effect circulation control for wind-turbine application considerations," Paper presented at the *Conference on Aerospace and Mechanical Engineering, World Engineering Congress 2010*, 2nd – 5th August 2010, Kuching, Sarawak, Malaysia.

[33] H. Djojodihardjo, M.F. Abdul-Hamid, S.N. Basri, F.F.I. Romli, and D.L.AS. Abdul-Majid, "Numerical simulation and analysis of Coandă effect circulation control for wind-turbine application considerations," *IIUM Engineering Journal*, Vol. 12, No. 3: Special Issue on Mechanical Engineering, 2011.

[34] COMSOL, Inc., *COMSOL 4.2: CFD Module User's Guide*, COMSOL, New England Executive Park, Burlington, Massachusetts, United States, 2011.

[35] H. Schlichting, *Boundary Layer Theory*, Translated by J. Kestin, McGraw-Hill, New York, 1979

[36] D. Kuzmin, O. Mierka, and S. Turek, "On the implementation of the k-e turbulence model in incompressible flow solvers based on a finite element discretization," *International Journal of Computing Science and Mathematics*, Vol. 1, No. 2–4, pp. 193–206, 2007.

[37] F.H. Harlow, and P. Nakayama, "Turbulence transport equations" *Physics of Fluids*, Vol.10, No.11, 1967.

[38] F.H. Harlow, and P. Nakayama, *Transport of Turbulence Energy Decay Rate*, LA-3854, UC-34, PHYSICS, TID-4500, Los Alamos Science Laboratory, University of California, 1968.

[39] B.E. Launder, A. Morse, W. Rodi, and D.B. Spalding, "The prediction of free shear flows - A comparison of the performance of six turbulence models," In: *NASA Langley Research Center Free Turbulent Shear Flows-Conference Proceedings*, Vol. 1, pp. 426, United States, 1973

[40] B.E. Launder, and B.I. Sharma, "Application of the energy-dissipation model of turbulence to the calculation of flow near a spinning disc," *Letters in Heat and Mass Transfer*, Vol. 1, No. 2, pp. 131-138, 1974.

[41] W.P. Jones, and B.E. Launder, "Predictions of low-Reynolds-number phenomena with a Z-equation model of turbulence," *International Journal of Heat & Mass Transfer*, p. 1119, 1973.

[42] W.P. Jones, and B.E. Launder, "The prediction of laminarization with a two-equation model of turbulence," *International Journal of Heat and Mass Transfer*, Vol. 15, pp. 314, 1972.

[43] J. Boussinesq, "Essai sur la théorie des eaux courantes," *Mémoires présentés par divers savants à l'Académie des Sciences*, Vol. 23, No. 1, pp. 1-680, 1877.

[44] C.L. Rumsey, and P.R. Spalart, "Turbulence model behavior in low Reynolds number regions of aerodynamic flow fields," Paper presented at the *38th AIAA Fluid Dynamics Conference and Exhibit*, Seattle, Washington, June 23-26, 2008.

[45] F.R. Menter, "Advances in Turbulence Modelling of Unsteady Flows", ANSYS, Germany, 2009; also Menter Shear Stress Transport Model, [Online]. Available: http:// turbmodels.larc.nasa.gov/sst.html

[46] D.C. Wilcox, *Turbulence Modeling for CFD*, 3rd Edition, DCW Industries, 2006.

[47] S. Benjanirat, *Computational Studies of Horizontal Axis Wind Turbines in High Wind Speed Condition using Advanced Turbulence Models*, Thesis(PhD), Georgia Institute of Technology, December 2006.

[48] S.M. Salim, and S.C. Cheah, "Wall y+ Strategy for Dealing with Wall-bounded Turbulent Flows," In: *Proceedings of the International Multi-Conference of Engineers and Computer Scientists 2009*, Vol. II, IMECS 2009, Hong Kong, March 18-20, 2009.

[49] T.D. Economon, and W.E. Milholen II, *Parametric Investigation of a 2-D Circulation Control Geometry*, Technical Report, Configuration Aerodynamics Branch Research and Technology Directorate, 2008.
[50] H. Grotjans, and F. Menter, "*Wall functions for general application CFD codes, ECCOMAS 98*," In: Proceedings of the 4th Computational Fluid Dynamics Conference, pp.1112-1117, 1998.
[51] D.M. Somers, *Design and Experimental Results for the S809 Airfoil*, NREL/SR-440-6918, UC Category: 1213, DE 97000206, National Renewable Energy Laboratory, Colorado, 1997.
[52] J. Abramson, and E.O. Rogers, *High-speed Characteristics of Circulation Control Airfoils*, AIAA-83-0265, David Taylor Naval Ship R&D Center, Aviation and Surface Effects Department, Bethesda, Maryland 20084, 1988.
[53] E.O. Rogers, *Development of Compressible Flow Similarity Concepts for Circulation Control Airfoils*, AIAA-87-0153, David Taylor Naval Ship R&D Center, Aviation and Surface Effects Department, Bethesda, Maryland 20084, 1987.